Available online at www.sciencedirect.com
SciVerse ScienceDirect
Procedia CIRP 4 (2012) 90 – 97
www.elsevier.com/locate/procedia

3rd CIRP Conference on Process Machine Interactions (3rd PMI)

# General Milling Stability Model for Cylindrical Tools

Zoltan Dombovari[a,]*, Jokin Munoa[b], Gabor Stepan[a]

[a]*Department of Applied Mechanics, Budapest University of Technology and Economics, Budapest 1521, Hungary*
[b]*Dynamics and Control Department, IK4-Ideko, Elgoibar, Basque Country, Spain*
* Corresponding author. Tel.: +36-1-463 1368; fax: +36-1-463 3471 .*E-mail address*: dombo@mm.bme.hu.

**Abstract**

In this study, the stability properties of general milling processes are summarized and compared to each other considering different special tool geometries. This general model can deal with any kind of flute geometry and with non-proportional damping using the semi-discretization method. A real-case experimental tip2tip modal analysis of a carbide milling tool is taken, which serves as the reference dynamics for the stability calculations. A fitting algorithm is used to extract the modal parameters of the corresponding non-proportionally damped system that is given directly in first order representation. The asymptotic stability of the stationary solution of the resulting time-periodic parametrically excited and time-delayed system is investigated by the semi-discretization algorithm. The stability properties of variable pitch, serrated and variable helix tools are compared with the one of the conventional helical tool.



*Keywords:* milling,;chatter; semi-discretization; delay; differential equation

## 1. Introduction

The use of proportional damping in the dynamic modeling of machine tools [1, 2] is a convenience approximation that makes the modal testing and also the related stability calculations and predictions easier. However, the traditionally acceptable approximation of proportional damping is usually unacceptable in these cases. Also, modal tests often present measurement results which cannot be fed into the time-domain based milling stability calculations [3, 4, 5, 6, 7] when accurate predictions are needed to optimize the material removal rate close to the stability limits. This is not a problem in case of frequency-domain methods [8, 9] that can cooperate directly with the measured frequency response functions (FRFs).

Another critical issue that makes existing stability predictions and chatter avoidance strategies questionable is the complex geometry of some recently designed milling tools, like the serrated ones or the ones variable pitch and/or variable helix [10, 11, 12, 13, 14, 15, 16, 29].

In this research report, the stability properties of the different special milling tools are compared in a case study where the experimental modal testing of a conventional carbide milling tool clearly presented non-proportional damping.

After a brief summary of the theoretical aspects, the modal testing of a MITSUBISHI AMMRD2000 tool is presented based on tip2tip measurement results. This leads to the construction of a realistic mathematical model that describes the regenerative effect with improved accuracy.

Then typical stability charts are presented for a varying pitch tool, for a serrated tool and for a varying helix tool (with non-uniform constant and harmonic variation). In the concluding section, the different kinds of stability improvements are compared for these cases. The otherwise intricate stability charts provide some essential observations regarding the primary parameter domains in the operational space of the cutting parameters where improved stability properties can be

 doi:10.1016/j.procir.2012.10.017

expected in the four cases compared to the case of a conventional milling tool.

## 2. Theory

First, those modeling issues are summarized, which are related to the cutter geometry and the cutting forces when general complex milling tools are considered. Then the linearized governing equations are compiled based on the machine tool dynamics in the presence of non-proportional damping and the corresponding stability calculation is presented for milling processes in general.

### *2.1. Geometric modeling of milling cutters*

There are many parameters to be used when the geometrical model of a general milling tool is constructed. Fig. 1 presents a summary of most of these parameters.

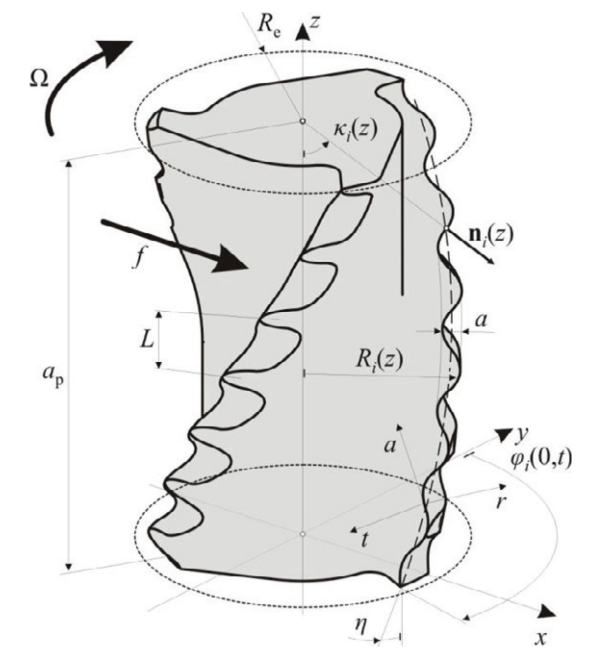

Fig. 1 shows the geometry of a general milling tool

The local lag angle $\varphi_{\eta,i}$ describes the angular-shift of the local edge segment due to the helix angle $\eta$ relative to the initial position angle of the $i$th edge at zero level $\varphi_i(0,t)$. Due to the possibly intricate helix variation, the local lag angle variation is given as

$$\varphi_{\eta,i}(z) = \varphi_{\overline{\eta},i}(z) - \delta_i(z), \quad i = 1,2,\ldots,Z, \qquad (1)$$

where $\varphi_{\overline{\eta},i}(z)$ is the mean lag angle, $\delta_i(z)$ is the introduced variation and $Z$ is the number of flutes. The lag angle is connected to the helix angle through the differential form

$$\varphi'_{\eta,i}(z) = \frac{1}{R_e}\tan\eta_i(z)\,, \qquad (2)$$

where $R_e$ is the envelope radius of the cylindrical tool. Thus, the envelope lead angle is $\kappa_e = 90$ deg. Using expression (2), the local helix angle can be calculated as

$$\eta_i(z) = \arctan(\tan\overline{\eta}_i - R_e\,\delta'_i(z))\,. \qquad (3)$$

The mean helix angles are $\overline{\eta}_i$ around which the actual helix angles $\eta_i(z)$ vary. The continuous variation of the helix angles cause variation in the pitch angle, too. This is described by the formula

$$\varphi_{p,i}(z) = \varphi_{p,i,0} + \varphi_{\eta,i}(z) - \varphi_{\eta,i+1}(z)\,, \qquad (4)$$

where $\varphi_{p,i,0} = \varphi_{p,i}(0)$ is the initial pitch angle at the axial level of $z = 0$.

Generally, the position angle of the $i^{th}$ local edge is given by (see Fig. 1)

$$\varphi_i(z,t) = \Omega t + \sum_{k=1}^{i-1}\varphi_{p,k}(z) - \varphi_{\eta,1}(z)\,, \qquad (5)$$

where $\Omega$ is the angular velocity of the tool. The serration is considered with the variation of the local radius $\Delta R_i(z)$ as

$$R_i(z) = R_e - \Delta R_i(z)\,. \qquad (6)$$

The local lead angle $\kappa_i(z)$ has a differential connection with the variation of the local radius:

$$\cot\kappa_i(z) = R'_i(z)\,. \qquad (7)$$

Assume that the actually trochoid-shape trajectories of tooth-segments can be approximated by circles. This is a standard approximation as opposed to the strict description of the edge trajectories presented in [17]. The assumption is appropriate if the feed per revolution is negligible compared to the essential diameter of the milling tool. If this condition is fulfilled then the expression of the cutting force can be related to the specific angular position $\varphi_i(z,t)$ of the 'just cutting' $i^{th}$ edge segment and the $(i+l)^{th}$ cutting edge segment that was at the same angular position some time earlier, when it cut the same surface segment at the time instant $t - \tau_{i,l}(z)$. Consequently, the following equality holds:

$$\varphi_i(z,t) = \varphi_{i+l}(z, t - \tau_{i,l}(z)) \,. \tag{8}$$

The continuous delay function $\tau_{i,l}(z)$ can be expressed with the help of the pitch angles (4) as

$$\tau_{i,l}(z) = \frac{1}{\Omega}\sum_{k=1}^{l-1} \varphi_{\mathrm{p},(i+k) \bmod Z}(z) \,. \tag{9}$$

The so-called geometrical chip thickness between the $i^{\mathrm{th}}$ and $(i+l)^{\mathrm{th}}$ flutes at level $z$ is

$$h_{\mathrm{g},i,l}(z,t) \approx \mathbf{r}_{i,l}(z,t)\,\mathbf{n}_i(z,t) \,, \tag{10}$$

where the movement of the edge segment during the time $\tau_{i,l}(z)$ is

$$\begin{aligned}\mathbf{r}_{i,l}(z,t) &= \mathbf{r}_i(z,t) - \mathbf{r}_{i+1}(z, t - \tau_{i,l}(z)) \\ &= \begin{bmatrix} (R_i(z) - R_{i+l}(z)) \sin\varphi_i(z,t) + f_{i,l}(z,t) \\ (R_i(z) - R_{i+l}(z)) \cos\varphi_i(z,t) \\ 0 \end{bmatrix} + \Delta\mathbf{r}_{i,l}(t)\end{aligned} \tag{11}$$

and the local normal vector (see Fig. 1) is defined as

$$\mathbf{n}_i(z,t) = \begin{bmatrix} \sin\kappa_i(z)\sin\varphi_i(z,t) \\ \sin\kappa_i(z)\cos\varphi_i(z,t) \\ -\cos\kappa_i(z) \end{bmatrix}. \tag{12}$$

The regeneration at (11) describes the connection between the present and the past motion of the tool:

$$\Delta\mathbf{r}_{i,l}(z,t) = \mathbf{r}(t) - \mathbf{r}(t - \tau_{i,l}(z)) \,. \tag{13}$$

The effective geometrical chip thickness is evaluated as the minimum of all possible geometrical chip thicknesses [18]

$$h_{\mathrm{g},i,e}(z,t) = \min_{l=1}^{Z} h_{\mathrm{g},i,l}(z,t) \,, \tag{14}$$

which can still be a negative number (theoretically). The effective index $e := e_i(z,t)$ varies digitally along the axial direction and shows if missed-cut effects arise during the cutting operation. The screen function $g$ takes into account the radial immersion and also the missed-cut effect if the following form is in use:

$$g_i(z,t) = \begin{cases} 1, & \left\{ \begin{array}{c} \varphi_{\mathrm{en}} < (\varphi_i \bmod 2\pi) < \varphi_{\mathrm{ex}} \\ \wedge \\ h_{\mathrm{g},i,e}(z,t) > 0, \end{array} \right. \\ 0, & \text{otherwise,} \end{cases} \tag{15}$$

where $\varphi_{\mathrm{en}}$ and $\varphi_{\mathrm{ex}}$ are the entry and exit angles measured clockwise from the $y$ axis (see Fig. 1). The physical chip thickness of the $i$th flute at level $z$ can be defined as

$$h_i(z,t) := g_i(z,t)\,h_{\mathrm{g},i,e}(z,t) \,, \tag{16}$$

which is already an always non-negetive value.

## 2.2. Resultant cutting force for general milling geometry

The cutting force per unit axial depth of cut (also called specific cutting force) at a particular edge location is expressed (see Fig. 1) in edge *tra* coordinate system as,

$$\mathbf{f}_{tra,i}(z,t) := -\mathbf{f}(h_i(z,t)) \,, \tag{17}$$

where $\mathbf{f}(h)$ is the empirical cutting force vector determined (measured) in tangential $t$, radial $r$, and axial $a$ directions as a function of the chip thickness. Here, for the sake of simplicity, only linear cutting force characteristics is considered in the following way

$$\mathbf{f}(h) = \mathbf{K}_{\mathrm{e}} + \mathbf{K}_{\mathrm{c}} h \,, \tag{18}$$

where $\mathbf{K}_{\mathrm{e}}=\mathrm{col}(K_{\mathrm{e},t}, K_{\mathrm{e},r}, K_{\mathrm{e},a})$ and $\mathbf{K}_{\mathrm{c}}=\mathrm{col}(K_{\mathrm{c},t}, K_{\mathrm{c},r}, K_{\mathrm{c},a})$ are the edge and cutting coefficients, respectively. The specific cutting forces are projected to the local spatial coordinate system $xyz$ with

$$\mathbf{f}_i(z,t,\mathbf{r}_t(\theta)) := -g_i(z,t)\,\mathbf{T}_i(z,t)\,\mathbf{f}_{tra,i}(z,t) \,, \tag{19}$$

where the transformation matrix $\mathbf{T}_i(z,t)$ can be found in [12]. Here, $\mathbf{r}_t(\theta) = \mathbf{r}(t+\theta)$, $\theta \in [-\sigma, 0)$ [19, 20] expresses the typically intricate regeneration properties (13), that can relate to several discrete delays in case of variable pitch angle tools [10, 14, 15] and serrated tools [11, 16] or to distributed delays in case of variable helix tools [13, 14, 16] ($\sigma$ is the maximum of occurring delays).

Basically the resultant cutting force $\mathbf{F}$ is the sum of the infinitesimal cutting forces along the edge portions that are in cut

$$\mathbf{F}(t,\mathbf{r}_t(\theta)) = \sum_{i=1}^{Z} \int_0^{a_{\mathrm{p}}} \frac{\mathbf{f}_i(z,t,\mathbf{r}_t(\theta))}{\cos\eta_i(z)\sin\kappa_i(z)} \mathrm{d}z \tag{20}$$

considering that the infinitesimal edge arc is $\mathrm{d}s_i = \mathrm{d}z/(\cos\eta_i(z)\sin\kappa_i(z))$.

## 2.3. Dynamics of the milling process

The governing equation of the milling process can be expressed in the spatial $xyz$ coordinate system as

$$\mathbf{M}\ddot{\mathbf{r}}(t)+\mathbf{C}\dot{\mathbf{r}}(t)+\mathbf{K}\mathbf{r}(t)=\mathbf{F}(t,\mathbf{r}_t(\theta)), \tag{21}$$

where **M**, **C** and **K** are the mass, damping and stiffness matrices, respectively. This formulism is not convenient when multiple modes arise in the structure, it needs to be transformed into the modal space. Since the system (21) can also be non-proportionally damped, that is, **C** cannot be expressed as a linear combination of **K** and **M**, a first order representation is considered as [21]

$$\mathbf{A}\dot{\mathbf{v}}(t)+\mathbf{B}\mathbf{v}(t)=\mathbf{Q}(t,\mathbf{v}_t(\theta)), \tag{22}$$

where the state vector is $\mathbf{v}(t)=\mathrm{col}(\mathbf{r}(t),\dot{\mathbf{r}}(t))$ and

$$\mathbf{A}=\begin{bmatrix}\mathbf{C} & \mathbf{M}\\ \mathbf{M} & \mathbf{0}\end{bmatrix},\ \mathbf{B}=\begin{bmatrix}\mathbf{K} & \mathbf{0}\\ \mathbf{0} & -\mathbf{M}\end{bmatrix},\ \mathbf{Q}=\begin{bmatrix}\mathbf{F}\\ \mathbf{0}\end{bmatrix}.$$

The system presented at (22) can be transformed immediately into the modal space of the $2n$ dimensional modal coordinate vector **q** defined by **v**=**Uq** even for non-proportional damping in the form

$$\dot{\mathbf{q}}(t)-[\lambda_k]\mathbf{q}(t)=\mathbf{U}^{\mathrm{T}}\mathbf{Q}(t,\mathbf{U}\mathbf{q}_t(\theta)). \tag{23}$$

This form of the equation of motion is independent from the spatial representation, thus, multiple modes can be considered with poles in the form of $\lambda_k=-\omega_{\mathrm{n},k}\,\xi_k+\omega_{\mathrm{d},k}\,\mathrm{i}$ and with the 'mass' normalized modal transformation matrix $\mathbf{U}=[\ldots,c_k\,\mathbf{p}_k,\ldots]$. The original mode shapes are $\mathbf{p}_k$, while $\omega_{\mathrm{n},k}$ and $\xi_k$ are the natural angular frequency and the damping ratio, respectively, and the damped natural frequency is denoted by $\omega_{\mathrm{d},k}=\omega_{\mathrm{n},k}(1-\xi_k^{\,2})$^(1/2). The normalization parameter is originated in the so-called modal scaling factor as $c_k^2=Q_k$. These modal parameters can be determined from experimental modal analysis using fitting algorithms assuming the following form for the FRF

$$\mathbf{H}(\omega)=\sum_{k=1}^{n}\left(\frac{Q_k\,\mathbf{p}_k\mathbf{p}_k^{\mathrm{T}}}{\mathrm{i}\omega-\lambda_k}+\frac{\bar{Q}_k\,\bar{\mathbf{p}}_k\mathbf{p}_k^{\mathrm{H}}}{\mathrm{i}\omega-\bar{\lambda}_k}\right), \tag{24}$$

where $n$ is the dimension of the second order representation (21).

### *2.4. Stability of the milling process*

The equation of motions of the considered general milling process at (23) is a parametrically excited delay differential equation (DDE) that is periodic at the principal period $T$. This principal period is originated from the tooth passing frequency $T$=2π/Ω/$Z$ in case of conventional milling, otherwise it is multiple times of 2π/Ω/$Z$ depending on the geometrical arrangement of the milling tool.

The solution of (23) can be separated to a stationary time-periodic part $\mathbf{q}_\mathrm{p}(t)=\mathbf{q}_\mathrm{p}(t+T)$ and to a perturbation $\mathbf{u}(t)$ as

$$\mathbf{q}(t)=\mathbf{q}_\mathrm{p}(t)+\mathbf{u}(t). \tag{25}$$

The asymptotic stability of the stationary solution $\mathbf{q}_\mathrm{p}$ can be determined through the variational equation [22] which has the form

$$\dot{\mathbf{u}}(t)=\mathbf{L}(t)\mathbf{u}(t)+\sum_{j=1}^{N_\tau}\mathbf{R}_j(t)\mathbf{u}(t-\tau_j), \tag{26}$$

where the coefficients are time-periodic: $\mathbf{L}(t)=\mathbf{L}(t+T)$ and $\mathbf{R}_j(t)=\mathbf{R}_j(t+T)$. Note that the variational equation (26) only contains discrete delays $\tau_j$ ($j$=1, 2, ..., $N_\tau$) due to the axial discretization of the cutting tool. In this case the originally continuous (distributed) delays defined at (9) are approximated by sufficiently large number of discrete delays.

Using the discretization process presented in [3, 23], the linear time-periodic DDE can be approximated by finite number of ordinary differential equations and the transition matrix **Φ** can be given in the form:

$$\mathbf{z}_{i+p}=\mathbf{\Phi}\,\mathbf{z}_i, \tag{27}$$

where the discretized state is $\mathbf{z}_i=\mathrm{col}(\mathbf{u}_i,\ldots,\mathbf{u}_{i-r})$, where $\mathbf{u}_{i-l}=\mathbf{u}(t_i-l\,\Delta\theta)$. The delay and the period resolution usually considered to be equal as $r=p$ and $r=\mathrm{int}(\sigma/\Delta\theta+1/2)$.

The stability of the stationary solution $\mathbf{q}_\mathrm{p}$ is determined with the help of the eigenvalues (characteristic multipliers) $\mu$ of the transition matrix **Φ**. If all characteristic multipliers have magnitude less than one then the stationary solution $\mathbf{q}_\mathrm{p}$ is asymptotically stable, otherwise, it is unstable.

## 3. Case study

In order to carry out the comparison of different milling tool geometries, a special case is considered with a milling tool of $Z$=3 flutes. The dynamics of the tool is taken from a real modal experiment performed on a MITSUBISHI AMMRD2000 tool with $L_\mathrm{s}$=105 mm overhang. The tip2tip measurements and the quality of the fitting algorithm are presented in Fig. 2. The extracted modal parameters can be found in Table 1.

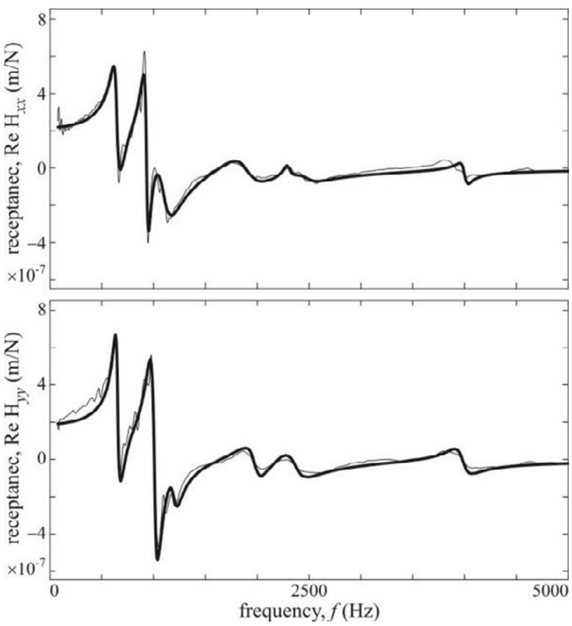


Fig. 2 shows the results of tip2tip FRF measurements (thin) and the result of the fitting process (thick).

During the application of the fitting algorithm, non-proportional damping was considered, which means that the mode shapes are complex vectors and the FRF can be presented in the form of (24).

Table 1 presents the extracted modal parameters using rational fraction polynomial method.

| $k$ | $\omega_{n,k}$ (Hz) | $\xi_k$ (%) | $Q_k$ ($10^4$ s/kg) | $\mathbf{p}_k$ |
|---|---|---|---|---|
| 1 | 646.5 | 5.34 | 0.89-0.90 i | $x$: −0.93+0.36 i |
| 2 | 935.0 | 2.65 | 0.18-1.33 i | $x$: −0.98+0.20 i |
| 3 | 1096.0 | 9.95 | 2.08-1.83 i | $x$: −0.89+0.45 i |
| 4 | 1893.8 | 8.47 | 1.41+0.35 i | $x$: 0.71-0.70 i |
| 5 | 2294.5 | 1.81 | −0.14+0.09 i | $x$: −0.06+0.99 i |
| 6 | 2482.9 | 5.20 | 0.35-0.14 i | $x$: 0.84-0.54 i |
| 7 | 4004.5 | 1.02 | 0.25+0.13 i | $x$: −0.44+0.90 i |
| 8 | 653.0 | 4.05 | 1.32-0.18 i | $y$: −0.81+0.59 i |
| 9 | 1008.1 | 3.54 | 2.40+0.58 i | $y$: 0.57-0.82 i |
| 10 | 1200.6 | 4.03 | −0.17-0.56 i | $y$: 1+0 i |
| 11 | 1985.0 | 4.20 | 0.70-0.61 i | $y$: −0.83+0.55 i |
| 12 | 2360.6 | 5.18 | 0.21-1.09 i | $y$: −1+0 i |
| 13 | 3979.6 | 2.13 | 0.65+0.31 i | $y$: 0.59-0.80 i |

For the stability calculations, simple quarter immersion down-milling is considered with simple straight cutting as a (desired) stationary cutting process. The parameters $K_{c,t}$ = 763.4 N/mm$^2$, $K_{c,r}$ = 110.8 N/mm$^2$ and $K_{c,a}$= 368.5 N/mm$^2$ are taken from the orthogonal to oblique [24, 25] model of Al7050T745 [11] considering mean helix angle $\eta$ = 37.5 deg.

Table 2 contains the basic geometrical data of the MITSUBISHI AMMRD2000 tool.

| | $Z$ | $D$ (mm) | $\eta$ (deg) | $a$ (mm) | $L$ (mm) |
|---|---|---|---|---|---|
|  | 3 | 20 | 37.5 | 0.67 | 3.25 |

## 4. Results

In order to compare the effect of different tool geometries, stability charts are calculated using the semi-discretization (SD) method in the parameter domain of spindle speed $\Omega\in[3000, 20000]$ rpm and depth of cut $a_p\in(0, 30]$ mm. The SD method was used with $N_{SD}$=90 elements in order to represent properly the delayed states $\mathbf{z}_i$ of the system.

The subsequent sections present the stability calculations and their results related to variable pitch tools, serrated cutters and variable helix tools with constant variations and also with harmonic ones.

### 4.1. Variable pitch cutter

In this section, cylindrical milling tools are considered with variable pitch only, that is,

$$\varphi_{p,i}(z) \equiv \varphi_{p,1}, \varphi_{p,2}, \ldots, \varphi_{p,Z-1}, \varphi_{p,Z}\,, \qquad (28)$$

where obviously

$$\varphi_{p,Z} = 2\pi - \sum_{i=1}^{Z-1} \varphi_{p,i}\,. \qquad (29)$$

Accordingly, only $N_\tau$=$Z$ pieces of discrete delays participate in the system dynamics through the regeneration (13).

In Fig. 3, one can follow how the variation of the pitch angle affects the linear stability of the corresponding milling process. As it was explained in [10], the variable pitch angles need to be optimized for certain milling operations in order to get large stability improvement as in Fig. 3$c$, otherwise the improvement may be moderate as in Fig. 3$a$. Generally speaking, variable pitch tools ensure moderate stability improvement at certain spindle speed regions only due to the redistribution of the instability lobe structure (cf. Fig. 3$a$ and Fig. 3$d$).

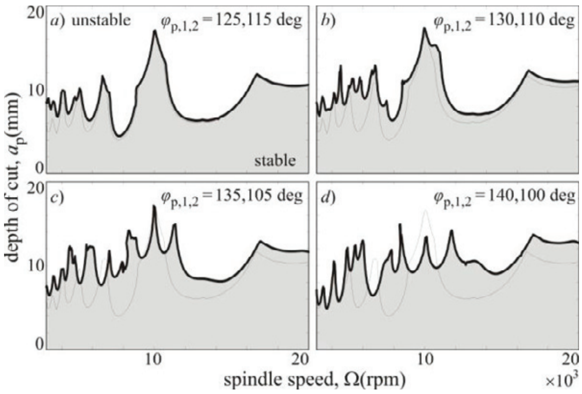


Fig. 3. Linear stability boundaries of milling operations performed with conventional tool (thin) and variable pitch tool (thick).

*4.2. Serrated cutter*

Since the experimental modal analysis was carried out on a serrated tool, the serration profile is defined by means of real scanned data [12]. The variation $\Delta R_i(z)$ introduced at (6) can be expressed by the dimensionless profile function $\rho(\zeta)$ as

$$\Delta R_i(z) = a\,\rho\left(\frac{z}{L} - \frac{\psi_i}{2\pi}\right), \qquad (30)$$

where $a$ is the peak-to-peak amplitude of the serration and the axial coordinate is scaled with the wavelength $L$ of the serration. The angle $\psi_i$ indicates the phase shift variation on the $i$th flute which is, in practice, uniformly distributed along the tool circumference:

$$\psi_i = (i-1)\varphi_p\,,\ i=1,\dots,Z. \qquad (31)$$

Here, $\varphi_{p,i}(z) \equiv \varphi_p$ represents the uniform pitch angle distribution. In this case, the maximum number of different discrete delays can be $Z$ in the dynamical model.

As it was explained in [12]**,** the stability improvement for a serrated cutter depends on the ratio of the applied feed $f$ and the peak-to-peak amplitude $a$. In order to characterize this, the so called dimensionless feed as $\varepsilon = f_Z/a$ is introduced, where $f_Z$ is the feed per tooth.

In Fig. 4, one can follow the effect of the feed variation on stability. The smaller feed is used the higher is the gain in stability. This phenomenon is completely opposite to the effect of the nonlinear cutting force characteristics where small feeds just destabilize the system [28]. In the series of figures from Fig. 4*a* to Fig. 4*d* one can follow how the linear stability limits are transformed from the stability boundaries of a fictitious one-fluted cutter to the three-fluted non-serrated tool's stability boundaries. The fact that this tool behaves as a one-fluted cutter makes the concept of a variable pitch serrated cutter meaningless, since in case of proper use, that tool would serve the same stability limits at relatively low feed. It can also be recognized that the above described transformation is not uniform, since up to $\varepsilon = 0.3$ the stability boundary remains roughly the same as for $\varepsilon = 0.01$ (see Fig. 4*ab*).

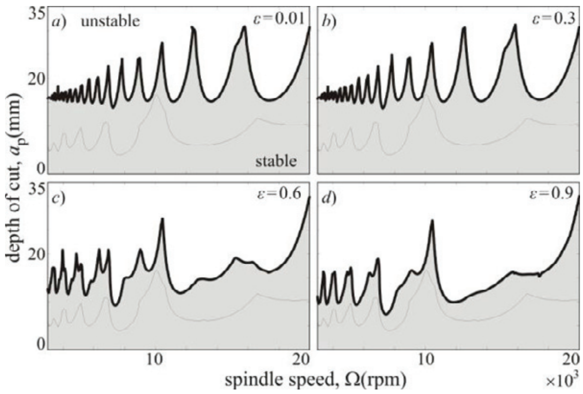


Fig. 4 shows the feed dependent linear stability boundaries of milling with conventional tool (thin) and with serrated tool (thick).

It is important to mention the obvious limitation of serrated cutters, namely, it can only be used in case of roughing operations. However, in roughing, these types of cutters require smaller drive torque due to the usually digressive cutting force characteristics against the chip thickness [12].

*4.3. Non-uniform constant helix tool*

These cutters are described by DDEs with distributed delays in which the delay intervals are weighted (see (9)). The effect is similar to the short regenerative effect that is one of the candidate theories to explain the so-called process damping in metal cutting that improves stability properties at low cutting speeds [26, 27].

In case of a cylindrical tool with non-uniform constant helix angle variation ($\overline{\eta}_i \equiv \eta_i$), the pitch angle is

$$\varphi_{p,i}(z) = \varphi_{p,i,0} + \frac{z}{R_e}(\tan\eta_i - \tan\eta_{i+1})\,, \qquad (32)$$

where uniform initial pitch angles are assumed, that is, $\varphi_{p,i,0} = 2\pi/Z$. A series of stability calculations are presented in Fig. 5, where one can realize that even a small deviation on the constant helix angles may cause improvements in stability especially in the low spindle speed zone.

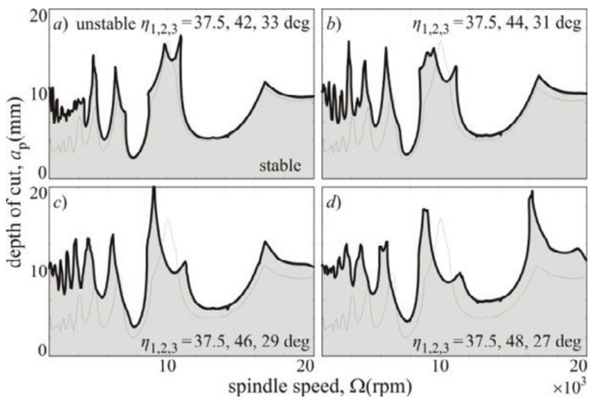


Fig. 5. Linear stability boundaries of milling for conventional tool (thin) and for non-uniform constant helix tool (thick)

The larger the deviation on the constant helixes is, the wider the zone where it improves the stability limits. It is important to note that these tools are already available in the market. Most of the tool manufacturers provide these kinds of solutions to improve the stability of milling processes, however, the deviation in helix is already set and those are usually small.

### 4.4. Harmonically varied helix tool

There are attempts to produce these kinds of complex milling cutters (see [16]), but generally it is difficult and expensive to grind the special edges and their performance has not been investigated thoroughly. These special edges induce also continuous distribution in the regeneration as the non-uniform constant helix tools. We consider uniform mean helix angles, that is, $\overline{\eta}_i \equiv \overline{\eta}$ for all edges. As it follows from (3) and (4), the harmonic variation of the helix angle is described by means of the pitch angles

$$\varphi_{\mathrm{p},i}(z) = \varphi_{\mathrm{p},i,0} + \delta_i(z) - \delta_{i+1}(z)\,, \tag{33}$$

where the variation $\delta$ is expressed as

$$\delta_i(z) = a_{\mathrm{h}}\ \sin\left(2\pi \frac{z}{L_{\mathrm{h}}} + \psi_{\mathrm{h},i}\right). \tag{34}$$

Thus, the pitch angle variation is expressed with the amplitude $a_{\mathrm{h}}$, the wavelength $L_{\mathrm{h}}$ and the phase shift $\psi_{\mathrm{h},i}$, which is considered to be uniform similarly to the case of serrated cutters in (31). The wavelength is kept to be $L_{\mathrm{h}}$=15 mm during the calculations.

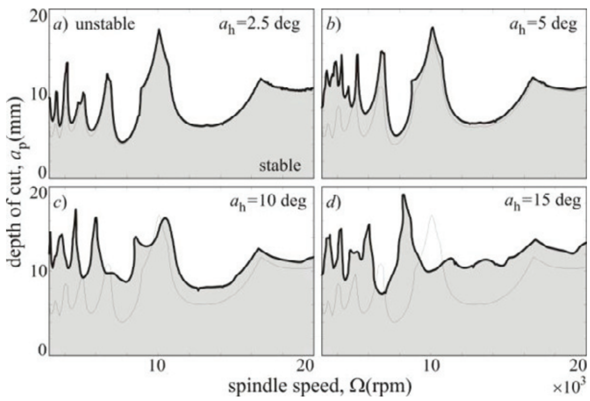


Fig. 6 shows how the harmonically varied helix tools affect the linear stability boundaries. The thin lines are the stability boundaries of an operation performed by a conventional tool.

In Fig. 6, the stability results are summarized with respect to the varied amplitude $a_{\mathrm{h}}$. The stability behavior of these cutters is similar to the one of the non-uniform constant helix tools. Small variation in the constant helix induces improvement of stability in the low spindle speed zone. The high speed zones are only affected when the tool has large amplitude variation. Note that large amplitude variation can be difficult to produce.

The effect of the wavelength is not analyzed here, because it is extremely difficult to machine small wavelength tools, while larger wavelengths would produce similar effect as the non-uniform constant helix angles do.

## 5. Conclusion

A general milling model is presented in this paper which makes it possible to describe different tool geometries including variable pitch, serration, and variable helix. Sample stability calculations were performed using real experimental tip2tip modal measurements. In the dynamical model, non-proportional damping was considered. The linear stability of the desired stationary milling processes was determined by means of the semi-discretization method.

The analysis showed that all of the techniques related to the discussed tool geometries can improve the stability behavior of milling processes compared to the milling process performed by conventional milling tools. Apart of the fact that it is only effective in case of roughing, the serrated cutters serve the largest stability improvement. While the variable pitch tools improve stability properties in certain spindle speed zones, the variable helix tools are effective in low spindle zones only if relatively small deviations are considered. Generally, the affected zones can be extended if larger deviations on the helices can be applied.

In case of serrated cutters, the improvement is guaranteed in case of proper use; however, all other techniques need certain optimization to achieve better performance than the one produced by conventional milling tools.

## 6. Acknowledgement

This work was supported by the Hungarian National Science Foundation under Grant No. OTKA K101714, and by the European FP7 Dynxperts project (260073/FP7-2010-NMP-ICT-FoF).

## References

[1] Tlusty, J., Spacek, L., 1954. Self-excited vibrations on machine tools, Nakl. CSAV (in Czech).
[2] Tobias, S., 1965. Machine-tool Vibration, Blackie, London, Glasgow.
[3] Insperger, T., Stepan, G., 2011. Semi-Discretization for Time-Delay Systems: Stability and Engineering Applications, Springer, New York.
[4] Bayly, P., Halley, J., Mann, B., Davies, M., 2003. Stability of interrupted cutting by temporal finite element analysis, Journal of Manufacturing Science and Engineering 125(2), p. 220–225.
[5] Khasawneh, F. A., Mann, B. P., 2011. A spectral element approach for the stability of delay systems, International Journal for Numerical Methods in Engineering 87, p. 566–592.
[6] Engelborghs, K., Luzyanina, T., Hout, K., Roose, D., 2000. Collocation methods for the computation of periodic solutions of delay differential equations, SIAM J. Sci. Comput. 22(5), p. 1593–1609.
[7] Roose, D., Szalai, R., 2007. Continuation and Bifurcation Analysis of Delay Differential Equations. Springer, Bristol, UK.
[8] Budak, E., Altintas, Y., 1998. Analytical prediction of chatter stability in milling—part I: General formulation, Journal of Dynamic Systems, Measurement, and Control 120(1), p. 22–30.
[9] Merdol, S. D., Altintas, Y., 2004. Multi frequency solution of chatter stability for low immersion milling, Journal of Manufacturing Science and Engineering 126(3), p. 459–466.
[10] Budak, E., 2003. An analytical design method for milling cutters with nonconstant pitch to increase stability, part I: Theory, Journal of Manufacturing Science and Engineering 125(1), p. 29–35.
[11] Merdol, S. D., Altintas, Y., 2004. Mechanics and dynamics of serrated cylindrical and tapered end mills, Journal of Manufacturing Science and Engineering 126(2), p. 317–326.
[12] Dombovari, Z., Altintas, Y., Stepan, G., 2010. The effect of serration on mechanics and stability of milling cutters, International Journal of Machine Tools and Manufacture 50(6), p. 511 – 520.
[13] Turner, S., Merdol, D., Altintas, Y., Ridgway, K., 2007. Modelling of the stability of variable helix end mills. International Journal of Machine Tools and Manufacture 47(9), p. 1410 – 1416.
[14] Sims, N., Mann, B., Huyanan, S., 2008. Analytical prediction of chatter stability for variable pitch and variable helix milling tools, Journal of Sound and Vibration 317(3-5), p. 664 – 686.
[15] Song, Q., Ai, X., Zhao, J., 2011. Design for variable pitch end mills with high milling stability, The International Journal of Advanced Manufacturing Technology 55, p. 891-903.
[16] Dombovari, Z., Stepan, G., 2012. The Effect of Helix Angle Variation on Milling, Journal of Manufacturing Science and Engineering (accepted), p. 1-9.
[17] Bachrathy, D., Stepan, G., Turi, J., 2011. State dependent regenerative effect in milling processes, ASME Computational and Nonlinear Dynamics 6(4), p. 041002.1–041002.9.
[18] Wang, J.-J., and Liang, S. Y., 1996. Chip load kinematics in milling with radial cutter runout, Journal of engineering for industry 118, p. 111–116.
[19] Hale, J., 1977. Theory of functional differential equations, Springer-Verlag, New York.
[20]Stepan, G., 1989. Retarded dynamical systems, Longman, London.
[21]Ewins, D., 2000. Modal Testing: theory, practice, and applications, Research Studies Press.
[22] Farkas, M., 1994. Periodic Motions. Springer-Verlag, Berlin and New York.
[23] Insperger, T., Stepan, G., 2002. Semi-discretization method for delayed systems, International Journal for Numerical Methods in Engineering 55, p. 503–518.
[24] Altintas, Y., 2000. Manufacturing Automation: Metal Cutting Mechanics, Machine Tool Vibrations, and CNC Design. Cambridge University Press, Cambridge.
[25] Budak, E., Altintas, Y., and Armarego, E. J. A., 1996. Prediction of milling force coefficients from orthogonal cutting data, J. Manuf. Sci. Eng 118, p. 216–225.
[26] Altintas, Y., Eynian, M., Onozuka, H., 2008. Identification of dynamic cutting force coefficients and chatter stability with process damping, CIRP Annals - Manufacturing Technology 57(1), p. 371–374.
[27] Bachrathy, D., and Stepan, G., 2010. Time-periodic velocity-dependent process damping in milling processes, in 2nd CIRP International Conference on Process Machine Interactions. Vancouver, Canada.
[28] Muñoa, J., Zatarain, M. Bediaga, I., Peigné, G. ,2006. Stability study of the milling process using an exponential force model in frequency domain, in CIRP-2nd International Conference High Performance Cutting (HPC), Vancouver, Canada.
[29] Yusoff, A. R., Sims, N.D., 2011. Optimisation of variable helix tool geometry for regenerative chatter mitigation. International Journal of Machine Tools & Manufacture 51(2), p. 133–141.